molecular pharmaceutics

Article

pubs.acs.org/molecularpharmaceutics

Lipophilic Decyl Chain–Pterin Conjugates with Sensitizer Properties

Mariana Vignoni,[†,‡] Niluksha Walalawela,[‡,§] Sergio M. Bonesi,[∥] Alexander Greer,[*,‡,§] and Andrés H. Thomas[*,†]

[†]Instituto de Investigaciones Fisicoquímicas Teóricas y Aplicadas (INIFTA), Departamento de Química, Facultad de Ciencias Exactas, Universidad Nacional de La Plata (UNLP), CCT La Plata-CONICET, Casilla de Correo 16, Sucursal 4, 1900 La Plata, Argentina

[‡]Department of Chemistry, Brooklyn College, City University of New York, Brooklyn, New York 11210, United States

[§]Ph.D. Program in Chemistry, The Graduate Center of the City University of New York, 365 Fifth Avenue, New York, New York 10016, United States

[∥]CIHIDECAR-CONICET, Departamento de Química Orgánica, FCEyN, Universidad de Buenos Aires, Pabellón 2, 3er Piso, Ciudad Universitaria, Buenos Aires, Argentina

Supporting Information

ABSTRACT: A new series of decyl chain [$-(CH_2)_9CH_3$] pterin conjugates have been investigated by photochemical and photophysical methods, and with theoretical solubility calculations. To synthesize the pterins, a nucleophilic substitution (S_N2) reaction was used for the regioselective coupling of the alkyl chain to the *O* site over the N^3 site. However, the *O*-alkylated pterin converts to N^3-alkylated pterin under basic conditions, pointing to a kinetic product in the former and a thermodynamic product in the latter. Two additional adducts were also obtained from an *N*-amine condensation of DMF solvent molecule as byproducts. In comparison to the natural product pterin, the alkyl chain pterins possess reduced fluorescence quantum yields (Φ_F) and increased singlet oxygen quantum yields (Φ_Δ). It is shown that the DMF-condensed pterins were more photostable compared to the N^3- and *O*-alkylated pterins bearing a free amine group. The alkyl chain pterins efficiently intercalate in large unilamellar vesicles, which is a good indicator of their potential use as photosensitizers in biomembranes. Our study serves as a starting point where the synthesis can be expanded to produce a wider series of lipophilic, photooxidatively active pterins.

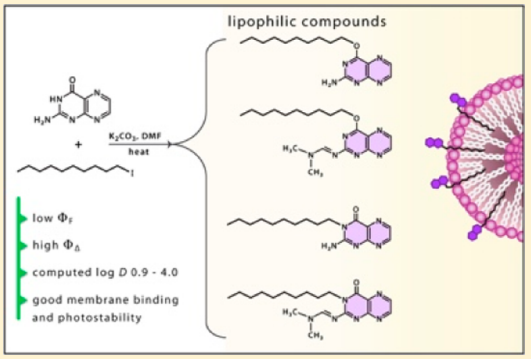

KEYWORDS: *lipophilic pterins, synthesis, fluorescence, singlet oxygen, LUVs*

INTRODUCTION

In 2016, a report showed that the natural product pterin (Ptr) freely passes across large unilamellar vesicles (LUVs) and photoinduces the oxidation of lipids of the membrane.[1] It was concluded that no direct contact existed between Ptr and the membrane, so that the photooxidation is a dynamic encounter process.[1] What was highlighted in this study is that pterins are not soluble in organic solvents and are only slightly soluble in water.

However, despite much research on pterins and much photochemical insight gained,[2−4] solubility problems have persisted. For this reason, we now report on how an alkylation approach, using decyl chain conjugation, provides avenues for studying pterins in lipophilic environments. Below, we first give background on pterin research to provide a sense of the state of pterin science.

Poor solubility has been a long-standing problem in pterin research. The synthesis of pterins can be cumbersome due to organic solvent insolubility so that column chromatography techniques are hampered. Only scarce reports exist on lipophilic pterins. Lipoidal biopterin (Bip) and tetrahydrobiopterin (H_4Bip) derivatives were synthesized to be used as prodrugs in diseases deficient in H_4Bip, such as phenylketonuria, Parkinson's disease, and Alzheimer's disease.[5] In addition, an *O*-alkylated 6-carbon chain at position 4 of a pterin derivative was synthesized for use as a redox-active wire targeting the pterin binding site of nitric oxide synthase.[6] However, except for the lipoidal Bip, there appear to be no other reports of long-chain alkylated pterins in the literature. The conjugation of long alkyl chains to drugs offers a handle for delivery to lipophilic sites. For example, a long-chain alkylated α-glucoside inhibitor 1-deoxynojirimycin increased its lipophilicity as well as its inhibitory potency.[7,8]

Special Issue: Pharmacology by Chemical Biology

Received: February 22, 2017
Revised: April 22, 2017
Accepted: May 2, 2017
Published: May 2, 2017

DOI: 10.1021/acs.molpharmaceut.7b00136
Mol. Pharmaceutics XXXX, XXX, XXX−XXX

In general, pterins are substituted at the 6 position (Scheme 1), bearing small substituents with 1 to 4 carbon atoms

Scheme 1

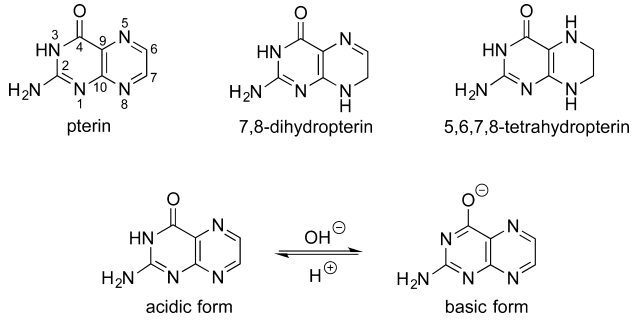

(unconjugated pterins) or larger substituents, such as the *p*-aminobenzoic acid (PABA) moiety (conjugated pterins) in folic acid (PteGlu).[9] Indeed, natural pterins exist in oxidized and reduced forms (Scheme 1). Pterins exhibit several dissociation equilibria, with the neutral (acid) form predominating at physiological pH (Scheme 1).

Upon UVA excitation (320−400 nm), unconjugated oxidized pterins present broad emission bands centered around 450 nm, fluorescence quantum yields (Φ_F) above 0.10, and fluorescence lifetimes (τ_F) in the range 2−14 ns.[10] On the other hand, conjugated pterins such as PteGlu show weak fluorescence (Φ_F < 0.01) because the PABA substituent acts as an "internal quencher" and deactivates the singlet excited states of the pterin moiety.

Oligodeoxynucleotides have been covalently bound to 6,7-diphenylpterin and used as photosensitizers.[12] Nucleoside analogues have been synthesized as pterin derivatives.[13] In the presence of oxygen, aromatic pterins act as photosensitizers through both type I (generation of radicals via electron transfer or hydrogen abstraction) and type II (production of $^1O_2$) mechanisms;[10,14] the former species (such as hydroxyl radicals) have very short diffusion distances, but the latter species $^1O_2$ can diffuse one hundred or more nanometers in biological media.[15,16] Pterins are reported to photosensitize oxidation of biomolecules, such as nucleotides,[17] DNA,[18] amino acids,[19] peptides,[20] proteins,[21,22] and biomembranes.[1] Relatedly, pterins have been found to induce the photokilling of cervical cancer (HeLa) cells upon UVA irradiation, and alter the integrity of the cell membranes, among other deleterious aspects.[23] Finally, the photodynamic inactivation of *Staphylococcus aureus* induced by carboxypterin has been recently demonstrated.[24] Nevertheless, synthetic methods for modifying pterins with a long alkyl chain, as has been done with drugs and dyes,[25−27] to better control solubilization and localization are needed to improve their versatility.

Here, we present a variation of the pterin topic to address the pterin solubility problem by the attachment of a straight chain of ten carbons. We thought a decyl−pterin conjugate would be a good target and bear a similar overall length to long-chain (C_{12}−C_{16}) fatty alcohols. The present study describes (1) the synthetic efficiency of pterin alkylation, (2) structural characterization and solubility, (3) pterins fluorescent quantum yields and singlet oxygen quantum yields, (4) photostability, and (5) phospholipid membrane binding data.

EXPERIMENTAL SECTION

Chemicals. Pterin (Ptr), 1-iododecane, dimethylformamide (DMF), dichloromethane (DCM), hexane, deuterated dimethyl sulfoxide (DMSO-d_6, 99.5%), and potassium carbonate (K_2CO_3) were obtained from Sigma and were used as received. Tris(hydroxymethyl)aminomethane (Tris) was provided by Genbiotech. L-α-Phosphatidylcholine from egg yolk (eggPC) and Sepharose CL-4B was bought from Sigma-Aldrich. Chloroform was from U.V.E., and acetonitrile and methanol were from J. T. Baker. All of them were HPLC grade. Water was purified using a deionization system.

Synthesis of Pterins 1−4. To a solution of Ptr (25 mg, 0.15 mmol) in DMF (12 mL) was added potassium carbonate (22 mg, 0.15 mmol). The mixture was sonicated and sparged with argon for 20 min. Then, 1-iododecane (65 μL, 0.3 mmol) was added to the solution. The reaction mixture was placed into a water bath and was stirred at 70 °C for 20 h. The solution was cooled at room temperature, and finally, the solvent was evaporated to dryness under vacuum, providing a solid residue. This solid residue was treated with NaCl (s.s.) (10 mL) and then was extracted with DCM (3 × 10 mL). The organic layers were separated, dried over Na_2SO_4, filtered, and evaporated to dryness. The white solid residue obtained was worked up by silica gel column chromatography (eluent: DCM 100% followed by DCM−methanol mixtures). From the eluted fractions, the products **1**−**4** were isolated and characterized by means of physical and spectroscopic methods. The first eluted fraction contained a mixture of products **1** and **2**, which were separated and purified by HPLC method. A Shimadzu HPLC apparatus with PDA and fluorescence detector was employed with a Synergi Polar-RP column (ether-linked phenyl phase with polar end-capping, 150 × 4.6 mm, 4 μm, Phenomenex) for product separation. The mobile phase was methanol, and the runs were carried out with a flow of 0.3 mL min^{-1}.

*4-(Decyloxy)pteridin-2-amine (**1**).* Yield: 17.5 mg (37%), purity 99%. R_f (methanol/DCM 5:95 v/v): 0.35. ^{1}H NMR (500 MHz, DMSO-d_6): δ 8.78 (d, J = 2 Hz, 1H), 8.43 (d, J = 2 Hz, 1H), 7.28 (s, 2H), 4.46 (t, J = 7 Hz, 2H), 1.81 (m, 2H), 1.23 (m, 14H), 0.84 (t, J = 7 Hz, 3H). ^{13}C NMR (100.6 MHz, DMSO-d_6): δ 166.9, 161.6, 157.2, 150.9, 139.5, 123.4, 67.2, 31.3, 29.0, 28.9, 28.7, 28.6, 28.1, 25.4, 22.1, 14.0. HRMS (ESI): m/z calcd for $C_{16}H_{25}N_5O$ [M + H^+] = 304.2137, found 304.2135.

*N′-(4-(Decyloxy)pteridin-2-yl)-N,N-dimethylformimidamide (**2**).* Yield: 17.5 mg (31%), purity 99%. R_f (methanol/DCM 5:95 v/v): 0.38. ^{1}H NMR (500 MHz, DMSO-d_6): δ 8.84 (s, 1H), 8.75 (d, J = 2 Hz, 1H), 8.50 (d, J = 2 Hz, 1H), 4.20 (t, J = 7 Hz, 2H), 3.26 (s, 3H), 3.13 (s, 3H), 1.65 (m, 2H), 1.24 (m, 14H), 0.85 (t, J = 7 Hz, 3H). ^{13}C NMR (100.6 MHz, DMSO-d_6): δ 161.3, 159.0, 157.4, 154.4, 149.9, 140.6, 130.0, 66.4, 42.5, 41.0, 35.0, 31.3, 28.9, 28.7, 27.4, 26.4, 22.1, 14.0. HRMS (ESI): m/z calcd for $C_{19}H_{30}N_6O$ [M + H^+] = 359.2559, found 359.2552.

*2-Amino-3-decylpteridin-4(3H)-one (**3**).* Yield: 9 mg (20%), purity 97%. R_f (methanol/DCM 5:95 v/v): 0.26. ^{1}H NMR (400 MHz, DMSO-d_6): δ 8.66 (d, J = 2 Hz, 1H), 8.36 (d, J = 2 Hz, 1H), 7.59 (s, 2H), 3.95 (t, J = 7 Hz, 2H), 1.56 (m, 2H), 1.23 (m, 14H), 0.85 (t, J = 7 Hz, 3H). ^{13}C NMR (100.6 MHz, DMSO-d_6): δ 160.7, 155.8, 153.9, 150.0, 139.1, 128.0, 41.7, 26.8, 31.3, 28.9, 28.8, 28.7, 26.0, 22.1, 14.0. HRMS (ESI): m/z calcd for $C_{16}H_{25}N_5O$ [M + H^+] = 304.2137, found 304.2134.

DOI: 10.1021/acs.molpharmaceut.7b00136
Mol. Pharmaceutics XXXX, XXX, XXX−XXX

*N′-(3-Decyl-4-oxo-3,4-dihydropteridin-2-yl)-N,N-dimethylformimidamide (**4**).* Yield: <1 mg (<1%), purity 99%. ^{1}H NMR (400 MHz, DMSO-d_6): δ 8.81 (s, H), 8.75 (d, J = 2 Hz, 1H), 8.48 (d, J = 2 Hz, 1H), 4.03 (t, J = 7 Hz, 2H), 3.23 (s, 3H), 3.10 (s, 3H), 1.63 (m, 2H), 1.25 (m, 14H), 0.85 (t, J = 7 Hz, 3H). HRMS (ESI): m/z calcd for $C_{19}H_{30}N_6O$ [M + H$^+$] = 359.2559, found 359.2556.

Absorption Measurements. Electronic absorption spectra were recorded on a Shimadzu UV-1800 spectrophotometer, using quartz cells of 0.4 or 1 cm optical path length.

pH Measurements. The pH was measured using a pH-meter sensION+ pH31 GLP combined with a pH electrode 5010T (Hach) or microelectrode XC161 (Radiometer Analytical). The pH of the aqueous solutions was adjusted by HCl and NaOH solutions. The concentration of the acid and the base used for this purpose ranged from 0.1 to 2.0 M.

Nuclear Magnetic Resonance. Spectra were recorded on a Bruker 400 MHz or a 500 MHz spectrometer operating at 400 MHz (or 500 MHz) for ^{1}H NMR and 100.6 MHz for ^{13}C NMR, using deuterated solvents.

Mass Spectrometry. The liquid chromatography equipment/mass spectrometry (LCMS) system was equipped with a UPLC chromatograph (ACQUITY UPLC from Waters) coupled to a quadrupole time-of-flight mass spectrometer (Xevo G2-QTof-MS from Waters) (UPLC-QTof-MS). UPLC analyses were performed using an Acquity UPLC BEH Shield RP18 column (1.7 μm; 2.1 × 100 mm) (Waters) and gradient elution staring with 20% water and 80% of methanol and finishing with 100% methanol, at a flow rate of 0.2 mL min^{-1}. The mass spectrometer was operated in positive mode with a capillary voltage of 2.5 kV, a cone voltage of 30 V, a cone gas flow of 20 L/h, the source temperature set to 130 °C, and the desolvation temperature set to 450 °C.

Fluorescence Measurements. Steady-state and time-resolved fluorescence measurements were performed at room temperature using single-photon-counting equipment FL3TCSPC-SP (Horiba Jobin Yvon), described elsewhere.[28] To obtain the fluorescence spectra, the sample solution in a quartz cell was irradiated with a CW 450 W xenon source through an excitation monochromator, and the luminescence, after passing through an emission monochromator, was registered at 90° with respect to the incident beam using a room-temperature R928P detector. In time-resolved experiments, a NanoLED source (maximum at 341 nm) was used for excitation, and the emitted photons, after passing through a monochromator, were detected by a TBX-04 detector and counted by a FluoroHub-B module. The selected counting time window for the measurements reported in this study was 0−200 ns.

The fluorescence quantum yields (Φ_F) were determined from the corrected fluorescence spectra using eq 1:

$$\Phi_F = \Phi_F{}^R I A^R / I^R A \quad (1)$$

where I is the integrated intensity, A is the absorbance at the excitation wavelength (λ_{exc}), and the superscript R refers to the reference fluorophore. In our experiments Ptr in alkaline media (Φ_F = 0.27)[10] and quinine bisulfate (Riedel-de Haën, Seelze, Germany) in 0.5 M H_2SO_4 (Φ_F = 0.546)[29] were used as reference. To avoid inner filter effects, the absorbance of the solutions, at the excitation wavelength, was kept below 0.10. Spectra were corrected for wavelength-dependent emission profiles with correction factors supplied by the manufacturer and using the software FluorEssence version 2.1 (Horiba Jobin Yvon).

Singlet Oxygen Measurements. For $^1O_2$ detection the experiments were carried out at room temperature using acetonitrile as a solvent since the lifetime of $^1O_2$ (τ_Δ) is long enough to detect it.[30] The $^1O_2$ emission in the near-infrared (NIR) region was registered using a NIR PMT Module H10330-45 (Hamamatsu) coupled to the equipment FL3 TCSPC-SP mentioned above, as described elsewhere.[17] Briefly, the sample solution (0.8 mL) in a quartz cell (1 cm × 0.4 cm) was irradiated with a CW 450 W xenon source through an excitation monochromator (330 nm blaze grating). The luminescence in the NIR region, after passing through an emission monochromator (1000 nm blaze grating), was detected at 90° with respect to the incident beam. Corrected emission spectra obtained by excitation at 350 nm were recorded between 950 and 1400 nm, and the total integrated $^1O_2$ phosphorescence intensities (IP) were calculated by integration of the emission band centered at ca. 1270 nm.

For determining quantum yields of $^1O_2$ production (Φ_Δ), the IP of each compound (IP^x) and that of phenalenone (IP^R) used as a reference sensitizer in the same solvent were measured, using matched absorbances at the wavelength(s) of excitation. Knowing the Φ_Δ of the reference ($\Phi_\Delta{}^R$) and assuming that the quenching of $^1O_2$ by the compounds **1**−**4** and by the reference sensitizer is negligible compared with $^1O_2$ deactivation by the solvent, the Φ_Δ value of a given compound x is given by eq 2.

$$\Phi_\Delta{}^x = \Phi_\Delta{}^R IP^x / IP^R \quad (2)$$

Steady-State Irradiation. The continuous photolysis of large unilamellar vesicles (LUVs) was carried out by irradiating in quartz cells (0.4 cm optical path length). Two Rayonet RPR 3500 lamps (Southern N.E. Ultraviolet Co.) with emission centered at 350 nm [bandwidth (fwhm) 20 nm] were employed as radiation source. Photolysis experiments were performed in air-equilibrated aqueous dispersions. Aberchrome 540 (Aberchromics Ltd.) was used as an actinometer for the measurement of the incident photon flux density ($q^{0,V}{}_{n,p}$) at the excitation wavelength.[31] The obtained value was 2.5 (±0.2) × 10^{-5} Einstein L^{-1} s^{-1}.

Preparation of LUVs. EggPC was dissolved in chloroform and dried under a nitrogen stream to form lipid films. Then the films were hydrated in Tris buffer (20 mM, pH 7.4). The samples were vortexed for a few minutes, and subsequently, the dispersions were sonicated using a probe sonicator (Sonics Vibra Cell, VCX750). EggPC LUVs were kept at 4 °C until used.

Molecular Exclusion Chromatography. The Sepharose CL-4B was equilibrated in 20 mM Tris pH 7.4 and poured into a 1.5 × 9 cm column. The gel was left sedimenting overnight. Samples were eluted with the same buffer and collected in 1 mL fractions.

LUVs Binding Experiments and Kinetics. To be sure the binding constant was obtained at equilibrium conditions, a kinetic experiment was carried out using a high concentration of LUVs (1.2 mM) and the corresponding pterin derivatives (2 μM). Fluorescence spectra were taken at different times, showing a small increase in fluorescence. No further significant increase in fluorescence was observed after 10 min of incubation; therefore binding constant measurements were performed incubating for at least 10 min.

Binding Constants. A titration method[32] was used to determine the binding constant (K_b). To a solution of the

DOI: 10.1021/acs.molpharmaceut.7b00136
Mol. Pharmaceutics XXXX, XXX, XXX−XXX

Scheme 2

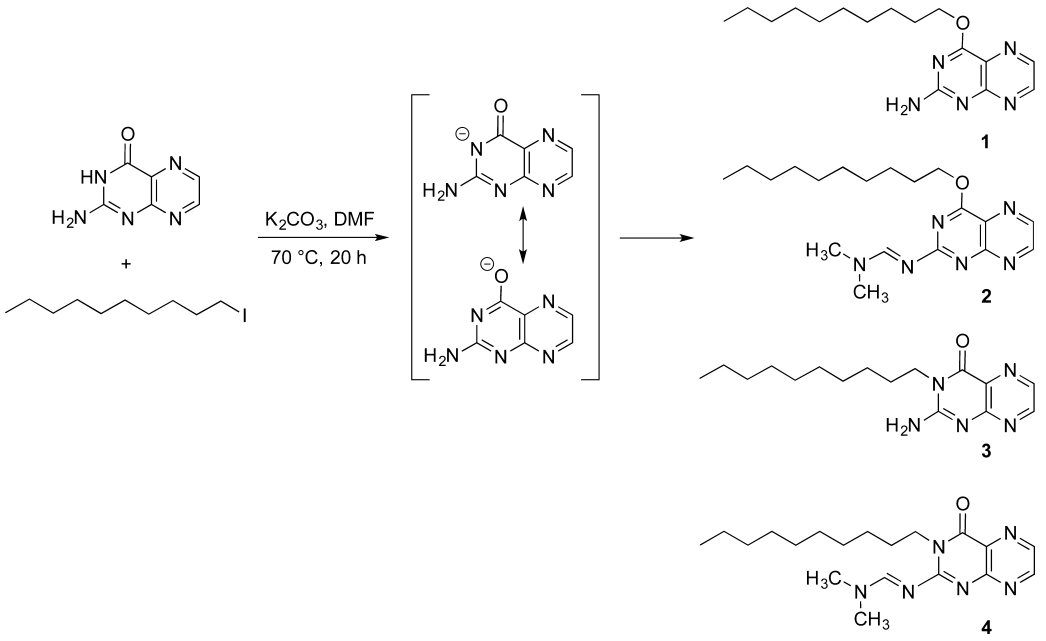

corresponding pterin derivative (2 μM) in buffer Tris, gradually increasing quantities of eggPC LUVs were added. The mixture was shaken and incubated for ~15 min, and the fluorescence spectrum was recorded. Corrected fluorescence spectra obtained by excitation at 341 nm were recorded between 390 and 600 nm, and the total fluorescence intensities (F) were calculated by integration of the fluorescence band between 410 and 600 nm. This parameter was then plotted on a graph against the lipid concentration and the data, and the following equation was used to fit the data:

$$F_L = F_0 + (F_\infty - F_0) \times [L]/(1/K_b + [L]) \quad (3)$$

where the three values F_0, F_L, and F_∞ are the fluorescence intensity of the compound without lipid, with lipid at concentration L, and that which would be obtained asymptotically at complete binding, respectively; and [L] is eggPC concentration.

Calculated Solubilities. Log P and log D values were computed with Marvin Sketch version 17.1.2 (ChemAxon Ltd. Budapest, Hungary).

RESULTS AND DISCUSSION

Synthesis and Characterization of Pterins 1−4. Our preparation of pterins **1**−**4** relied on the use of basic reaction conditions and 1-iododecane as the alkylating reagent in *N*,*N*-dimethylformamide (DMF) at 70 °C (Scheme 2). Fortunately, the alkylation enhanced product solubility enabling the separation of **1** in 37%, **2** in 31%, **3** in 20%, and **4** in <1% overall yields. Based on HPLC data, the purity of **1** was 99%, of **2** was 99%, of **3** was 97%, and of **4** was 99%. The alkylated pterins were easily separated. LCMS data indicated that **1** and **3** each contained one decyl chain (for **1** the MS calcd for $C_{16}H_{25}N_5O$ [M + H$^+$] = 304.2137, found 304.2135; for **3** the MS calcd for $C_{16}H_{25}N_5O$ [M + H$^+$] = 304.2137, found 304.2134). LCMS data indicated that **2** and **4** contained a decyl chain and a condensed DMF molecule (for **2** the MS calcd for $C_{19}H_{30}N_6O$ [M + H$^+$] = 359.2559, found 359.2552; for **4** the MS calcd for $C_{19}H_{30}N_6O$ [M + H$^+$] = 359.2559, found 359.2556). ^{1}H NMR data led us to the regiochemical assignments of **1**−**4**. The 1-CH_2 proton signals for the *O*-alkylated pterins are assigned for **1** at 4.35 ppm and for **2** at 4.20 ppm, whereas 1-CH_2 proton signals of N^3-alkylated are assigned for **3** at 3.95 ppm and for **4** at 4.03 ppm due to the methylene group attached to the more electronegative oxygen than nitrogen atom.

At 70 °C, there was regioselectivity for *O*-alkylation compared to N^3-alkylation. However, in the presence of base (1 M NaOH) the *O*-alkylated pterins convert to N^3-alkylated pterins. Thus, there is evidence that pterins **1** and **2** are kinetic products, and pterins **3** and **4** are thermodynamic products, by analogy to tautomer structures of purines, as well as thermodynamic *N*-alkylated purines with quinone methides.[33,34] Here, aromaticity does not appear to be a driving force for formation of **1** and **2** relative to **3** and **4**, as has been found for other rearrangements and product formation.[35,36] No evidence was found for the formation of dialkylated pterins, which may be explained by the high energy costs by steric shielding once the first alkyl chain is added there by prohibiting the addition of the second alkyl chain. As an aside, pterins **2** and **4**, which have the condensed DMF molecules, are somewhat structurally similar to biguanide derivatives with NH_2−C(NH)−NH−C(NH)−NH_2 groups, such as the antidiabetic drug metformin.[37−41] Next, our decyl−pterin conjugates **1**−**4** were evaluated for their solubility and photosensitizer properties.

Solubility. Our alkylation process leads to pterins that are soluble in organic solvents. Experimental and computational data indicate that addition of the decyl chain to pterins led to organic solvent solubility, instead of the water solubility seen in the parent Ptr. Pterins **1**−**4** were found to have high solubility in organic solvents, such as dichloromethane, dimethyl sulfoxide, acetonitrile, and methanol. By comparison, unsubstituted pterins are insoluble in organic media and sparingly soluble in water, e.g., 2 mg of Ptr dissolves in 100 g of water (22 °C). Alkaline conditions (e.g., 0.05 M NaOH)[42] can allow for greater solubility, or solvent mixtures must be used, such as 1:1 ratios of methanol/water or DMSO/water.

DOI: 10.1021/acs.molpharmaceut.7b00136
Mol. Pharmaceutics XXXX, XXX, XXX−XXX

Table 1 shows computed log *P* and log *D* data for the pterins in the series to predict the partitioning in lipophilic media. Log

Table 1. Computed Log *P* and Log *D*

compd	computed log P^a	computed log D^a pH 3	pH 7	pH 11
1	3.53	3.52	3.53	3.53
2	3.97	2.23	3.95	3.97
3	2.81	2.81	2.81	2.81
4	2.92	0.89	2.66	2.92
pterin		−0.96	−0.16	−1.96

[a]Computed with the MarvinSketch 17.1.2 (ChemAxon Ltd. Budapest, Hungary).

P is the partition coefficient of a neutral pterin, and log *D* is the distribution coefficient for the partitioning of charged pterins. Both log *P* and log *D* are computed for relative pterin partitioning in biphasic media. Clearly, the addition of the decyl chain leads to higher octanol solubility for the *O*-alkylated pterins **1** and **2** compared to N^3-alkylated pterins **3** and **4**. Thus, pterins **1** and **2** may exhibit greater binding than **3** and **4** in membrane and lipid environments. The computed log *D* data are equal to the appropriate values of log *P* for pterins **1** and **3** between pH 3 and 11. This suggests that pterins **1** and **3** are resistant to dissociation in an acidic or basic medium. However, log *D* values of biguanide-like pterins **2** and **4** deviate from corresponding log *P* in acidic pH. On the other hand, the parent Ptr in the neutral or anionic state was predicted to have water solubility rather than octanol solubility. The negative computed log *D* values for basic and acidic pterin are due to their water solubility, in particular for the former the basic pterin. The conjugation of the alkyl chain to pterin led to increased solubility in lipophilic media for further testing, as we will see next.

Absorption and Emission Spectra. Figure 1 shows the absorption spectra for the compounds **1**−**4** in acetonitrile,

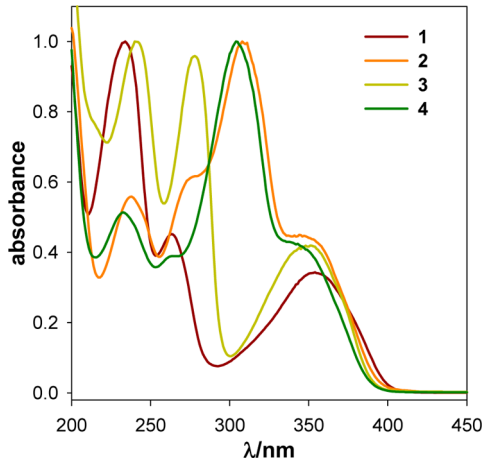

Figure 1. Absorption spectra of pterins **1**−**4** in acetonitrile. Spectra are normalized at the absorption maximum of each compound.

which were very similar to those recorded in methanol. Compounds **1** and **3** have a broad band centered at ca. 350 nm, similar to the typical UVA band of Ptr.[10] Compounds **2** and **4** have an intense absorption band centered about 305 nm, which is not present in the Ptr spectrum and can be attributed to the condensed DMF moiety. This band is partially superimposed to the typical UVA absorption band of Ptr.

Pterins **1**−**4** were dissolved in 1:1 (v/v) methanol/water mixtures, and their corresponding absorption spectra were recorded at two different pHs (5 and 10), since the pK_a of Ptr is ∼8. No pH dependence was observed for **1**−**4**, suggesting that the typical acid−base equilibrium of the Ptr moiety is not present. This fact is in agreement with the proposed structures, since the acid−basic equilibrium is lost due to the alkylation (Scheme 1). Furthermore, the absorption spectra of pterins **1** and **3** were compared with the acid and basic forms of Ptr in aqueous solution:[43] compound **1**, which has the same structure of basic Ptr, has the high energy band blue-shifted in comparison with the corresponding band of compound **3** (structure similar to acid Ptr), and the low-energy band of compound **1** is red-shifted in comparison with the corresponding band of compound **3**. Therefore, the spectral features of compounds **1** and **3** are logical taking into account the proposed chemical structures (Scheme 1).

Figure 2 shows the corrected fluorescence spectra by excitation at 350 nm of compounds **1**−**4** in acetonitrile. The

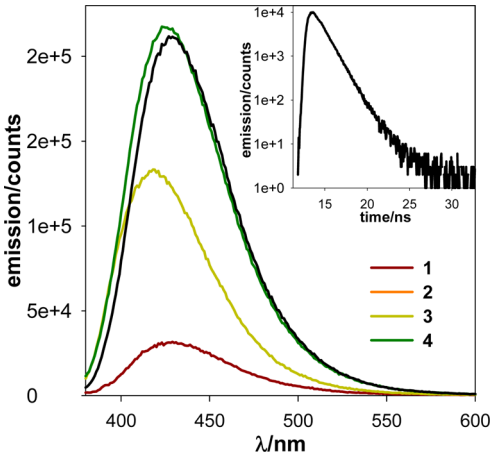

Figure 2. Fluorescence emission spectra of pterins **1**−**4** in acetonitrile. The absorbance of all compounds was equal at 350 nm. Inset: fluorescence decay of pterin **2** (λ_{exc} = 341 nm, λ_{em} = 430 nm).

emission maxima are blue-shifted compared to the corresponding Ptr spectrum in aqueous solutions (Table 2). Furthermore, the fluorescence quantum yields (Φ_F) were determined (Table 2), and all of them were lower than those previously reported for Ptr.[43] A first-order rate law was observed for all the emission decays. A typical trace recorded for pterin **2** is shown in Figure 2. Fluorescence lifetimes (τ_F) were determined to be around 1.5 ns, which is significantly lower than those reported for Ptr and other unconjugated oxidized pterins.[11,43] These values explain why Φ_F of compounds **1**−**4** are lower than that reported for Ptr and reveal that the chain linked to the pterin moiety enhances the deactivation of the singlet excited state.

Singlet Oxygen Production. Pterins **1**−**4** were found to generate $^1O_2$ in air-equilibrated acetonitrile solutions by monitoring its near-infrared luminescence at 1270 nm. Figure 3 shows $^1O_2$ emission that was detected for each pterin. To our delight, pterins **1**−**4** yielded higher Φ_Δ values compared to the parent pterin (Table 2).[44]

It is important to recall that conjugated pterins, e.g., folic acid, are poor $^1O_2$ sensitizers[10] and present very low Φ_F values due to internal fluorescence quenching by rapid radiationless

DOI: 10.1021/acs.molpharmaceut.7b00136
Mol. Pharmaceutics XXXX, XXX, XXX−XXX

Table 2. Spectroscopic Properties of Pterins 1−4 in Acetonitrile[a]

compd	λ_{max}/nm absorption	λ_{max}/nm emission	fluorescence quantum yield[b] $\Phi_F \pm$ SD	fluorescence lifetime/ns[c] $\tau_F \pm$ SD	$^1O_2$ quantum yield[d] $\Phi_\Delta \pm$ SD
1	234/263/354	428	0.012 ± 0.002	1.2 ± 0.2	0.50 ± 0.02
2	238/309	428	0.078 ± 0.008	1.5 ± 0.1	0.37 ± 0.02
3	240/278/348	417	0.043 ± 0.005	0.8 ± 0.1	0.36 ± 0.02
4	232/305	424	0.076 ± 0.008	1.5 ± 0.1	0.35 ± 0.01
parent Ptr (basic form)[e]	252/358	456	0.27 ± 0.02	5.0 ± 0.4	0.30 ± 0.02
parent Ptr (acidic form)[e]	270/340	439	0.33 ± 0.02	7.6 ± 0.4	0.18 ± 0.02

[a]Wavelengths of absorption and fluorescence (λ_{max}), fluorescence quantum yields (Φ_F), fluorescence lifetimes (τ_F), and singlet oxygen quantum yields (Φ_Δ). [b]λ_{exc} 350 nm. [c]λ_{exc} 341 nm, λ_{em} 420−430 nm. [d]λ_{exc} 350 nm. [e]Solvent: water, data from ref 11.

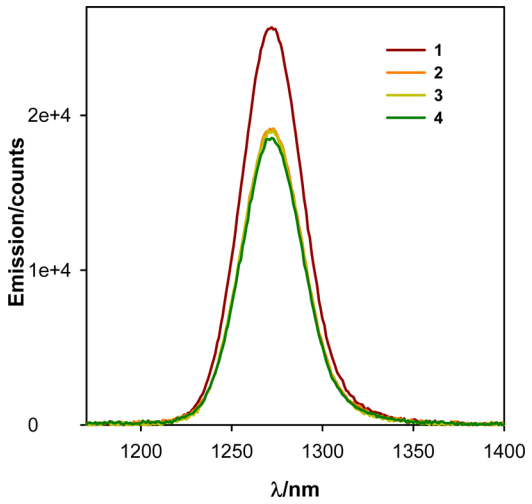

Figure 3. Singlet oxygen emission spectra of pterins **1**−**4** in acetonitrile (λ_{exc} = 350 nm).

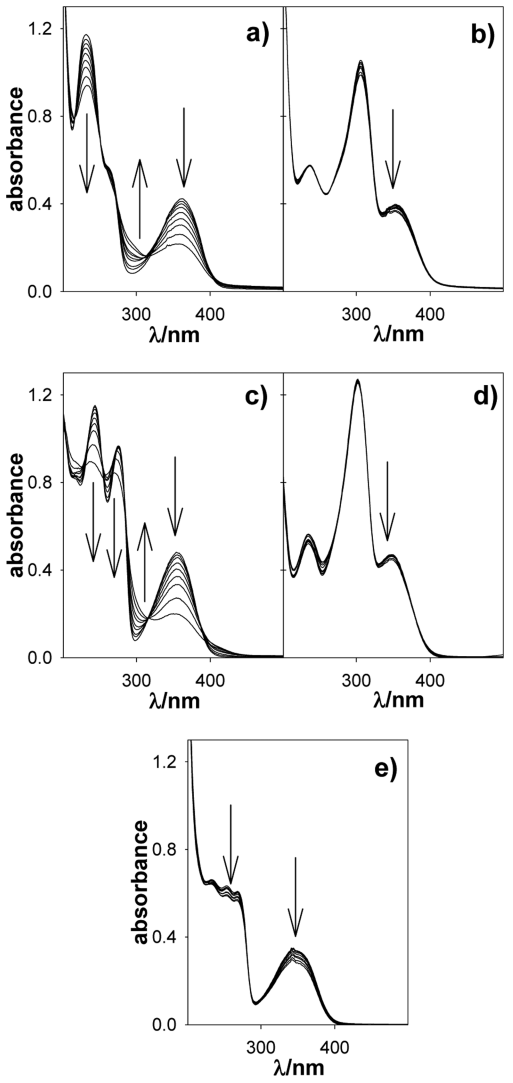

Figure 4. Time evolution of the absorption spectra of irradiated solutions of (a) pterin **1**, (b) pterin **2**, (c) pterin **3**, (d) pterin **4**, and (e) Ptr. Spectra were recorded at 0, 5, 10, 20, 30, 45, 60, 90, 120 min. The optical path length was 1 cm. Arrows indicate changes observed (λ_{exc} 350 nm).

deactivation of the singlet excited state.[11] This deactivation process is thought to occur through an intramolecular electron transfer between the PABA moiety and the singlet excited state of the pterin moiety.[45] The behavior observed for pterins **1**−**4** is different and indicates that the decyl chain substituent, in this case, does not enhance the deactivation of the singlet excited state to the ground state. Indeed, this is logical because an intramolecular electron transfer is not possible from the decyl chain substituent. Moreover, the low Φ_F values for **1**−**4** compared to Ptr are attributed to efficient intersystem crossing, and consequently higher Φ_Δ values. We show that the decyl chain substituent in pterins **1**−**4** not only leads to higher solubility in organic solvents but also preserves the capacity to form triplet excited states and therefore function as $^1O_2$ photosensitizers.

Photostability. In addition to increased singlet oxygen quantum yields, protection of the pterin from photodegradation would be desired for its use as a photosensitizer. Therefore, we investigated the photostability of pterins **1**−**4**. Solutions of each compound were exposed to UVA irradiation, and the corresponding absorption spectra were recorded at different times. Deep spectral changes were observed for pterins **1** and **3** in the first 30 min of irradiation (Figure 4a and 4c) revealing that, under our experimental conditions, these compounds are rapidly photodegraded. On the other hand, pterins **2** and **4** seem to be much more photostable, since almost no spectral changes were registered in 2 h of irradiation (Figures 4b and 4d). For comparative purposes photolysis of Ptr under the same conditions was carried out. Results showed that Ptr was slightly degraded within the time window of the experiment (Figure 4e). In other reports,[46−50] sensitizers or compounds with free amine groups have been shown to be labile to photodegradation, often occurring through a type I (electron transfer and H atom abstraction) photosensitized reac-

DOI: 10.1021/acs.molpharmaceut.7b00136
Mol. Pharmaceutics XXXX, XXX, XXX−XXX

tion.[14,51,52] Knowledge of synthetically modified pterins for higher stability to photooxidative stress is very useful.

Membrane Binding. As we mentioned in the Introduction, a previous report showed that Ptr crosses lipid biomembranes (LUVs) and is not intercalated to the membrane for any significant period of time.[1] To study whether the long-chain pterins can interact with lipid membranes, studies similar to those described in ref 1 were performed. Pterins **1** and **2** were chosen since their high percent yields allowed us to obtain sufficient quantities for lipid interaction studies. EggPC LUVs containing 2% of each compound were passed through a size exclusion chromatography column. Fractions were collected and analyzed by spectrophotometry, to detect the light scattering of LUVs, and by fluorescence spectroscopy, to detect pterins **1** and **2**. Figure 5 shows that LUVs eluted

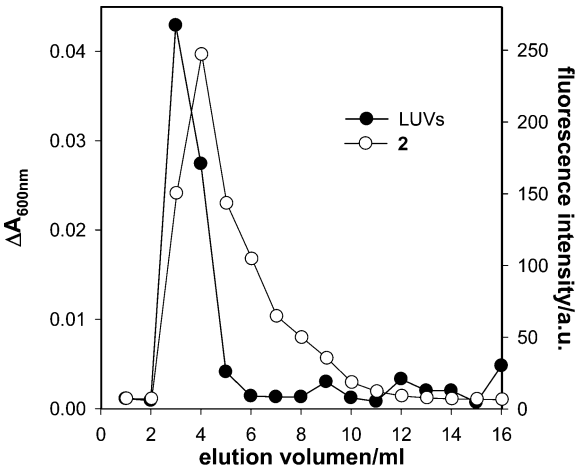

Figure 5. Elution profiles of molecular exclusion chromatography performed on eggPC LUVs from free pterin **2**. The absorbance at 600 nm (●) and the fluorescence intensity (○) was registered for each fraction to detect the LUVs and pterin **2**, respectively (λ_{exc} 340 nm).

between fractions 4 and 6, which are the same fractions where pterin **2** was detected. The same behavior was observed for pterin **1**. This result indicates that our decylpterins can intercalate to the membranes. Since no emission was detected in any other fraction of the chromatography column, that is, no free compound was observed, we surmise that the intercalation of pterins **1** and **2** to lipid biomembrane was close to 100%.

To quantify the interaction of pterins **1** and **2** with biomembranes (eggPC LUVs), we carried out titration curves at a constant concentration of a given pterin derivative and increasing concentration of lipid (Experimental Section), and the corresponding binding constants (K_b) were determined. To guarantee that the LUVs:pterin system was at equilibrium, the emission spectra of the mixtures corresponding to the maximum concentration of lipids used for each titration curve were monitored for up to 1 h. For both pterin derivatives no significant changes were observed after 10 min of incubation, indicating that the system had reached the equilibrium. Therefore, all measurements of the titration curves were performed after 15 min of incubation. Figure 6 shows the emission spectra of pterins at different eggPC concentrations. Fluorescence emission of pterin **1** decreased with the increase of eggPC concentration while the opposite happened for pterin **2**. Binding constants of pterins to LUVs were obtained fitting the fluorescence intensity as a function of the concentration of eggPC (Figure 7). Values of K_b obtained for pterin **1** and **2** are

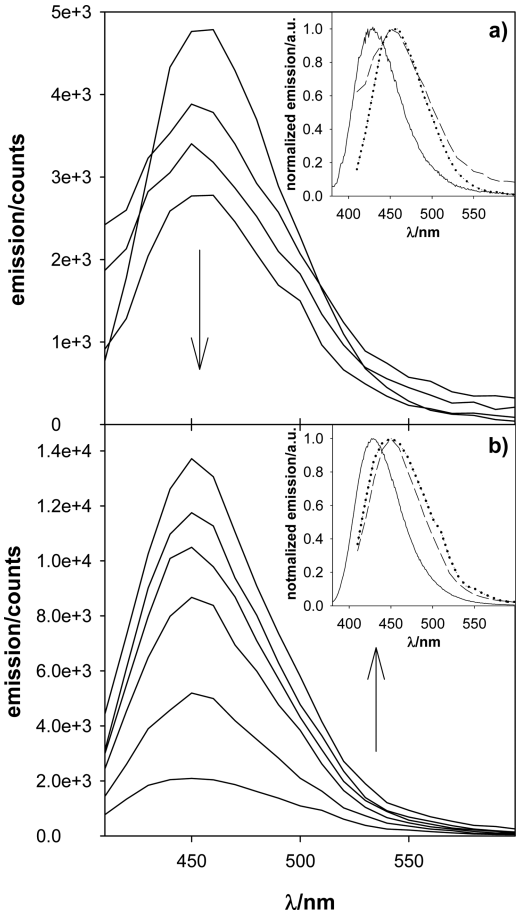

Figure 6. Fluorescence emission spectra of pterins (a) **1** and (b) **2** as a function of eggPC LUVs addition (arrows indicate increase in eggPC concentration). Inset: Normalized fluorescence emission spectra in acetonitrile (−), in aqueous media (···), and in lipid biomembranes (− − −) (λ_{exc} 340 nm).

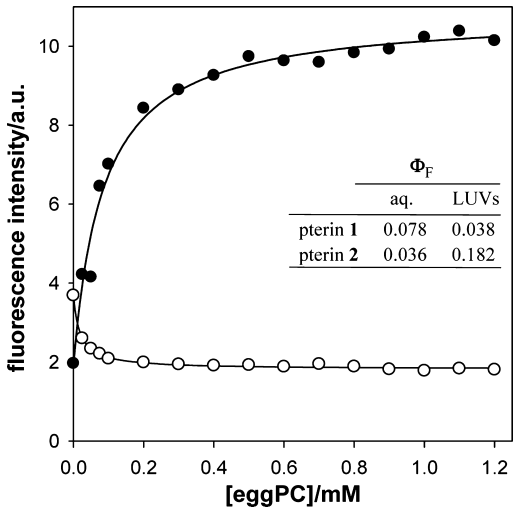

Figure 7. Association of pterins **1** (○) and **2** (●) in eggPC LUVs.

4 (±1) × 10^4 and 1.1 (±0.3) × 10^4 M^{-1}, respectively, which are in the same order of constants obtained for other dyes such as xanthenes[53] or porphyrins.[32]

The emission spectra of pterins **1** and **2** in the absence of LUVs were used to calculate the corresponding Φ_F values in aqueous media (inset Figure 7), which, in agreement with

DOI: 10.1021/acs.molpharmaceut.7b00136
Mol. Pharmaceutics XXXX, XXX, XXX−XXX

measurements performed in ACN, were significantly lower than those reported for parent pterin in water (Table 2). In the same way, the emission spectra of pterins **1** and **2** at high eggPC concentrations (e.g., [eggPC] ≥ 1 mM), where the fraction of free compounds is negligible, were used to estimate the Φ_F values in LUVs (inset Figure 7), which were again much lower than those reported for parent pterin.

It is noteworthy that normalized fluorescence spectra of pterins **1** and **2**, in the absence of LUVs, are shifted to longer wavelength when compared to the corresponding spectra of compounds in acetonitrile (inset Figure 6). On the other hand, normalized fluorescence spectra of pterins **1** and **2** in water compared to residing via intercalation in the biomembranes (high concentration of eggPC) are almost equal, which suggests that the fluorophore of each compound (pterin moiety) anchored to the biomembrane is in an aqueous environment. This fact allows us to hypothesize that, whereas the decyl substituent is intercalated deep in the lipid bilayer and is responsible for the interaction, the pterin moiety is in the outer, protic and polar region of the biomembrane.

CONCLUSION

Decyl chain conjugation to pterins dramatically increases their lipophilicity, which is pertinent to their photoactivity and photostability. The following conclusions are made: (1) Decyl chain pterin conjugates were synthesized in a regioselective manner. At 70 °C, the *O*-alkyl pterins are formed in higher yield than the N^3-alkyl pterins. However, the *O*-alkyl pterins (kinetic species) are converted to N^3-alkyl pterins (thermodynamic species) under basic conditions. Only one mole of iododecane was added to pterin. Addition of two moles of iododecane for dialkylated pterins was not seen. (2) Conjugation of the decyl chain in pterin increases solubility in organic solvents. Within this series, log *P* values for **1** and **2** suggest slightly higher lipophilicity compared to **3** and **4**. (3) Pterins **1**−**4** are shown to be $^1O_2$ sensitizers. We show that the new pterins have higher $^1O_2$ quantum yields compared to Ptr, implying greater photooxidative activity. The fluorescent quantum yields for the pterins **1**−**4** are relatively modest, and thus do not point to utility as fluorescent probes. (4) Generating high-stability pterins resistant to self-photooxiation is an advantage. The condensed DMF molecules conferred photostability to pterins **2** and **4** compared to **1** and **3** and Ptr itself that bore free amine groups. (5) Pterins **1** and **2** intercalate in biomembranes with binding constants comparable to those of xanthenes and porphyrins.

The new pterins can be advantageous compared to natural pterins that readily pass through membranes. Further efforts in synthesis can lead to additional lipophilic and photoactive pterins with relative ease, which will be important in future research. A benefit of a long-chain pterin is that it can increase in detergent-like and amphiphilic properties, also a desirable feature in making nanovesicles. We are now developing reactions for pterins as liposomes, i.e. "ptersomes", which we aim to report in the near future. Porphyrin-based conjugation routes have already emerged for porphysome nanovesicles with use in photothermal therapy.[54−58]

ASSOCIATED CONTENT

Supporting Information

The Supporting Information is available free of charge on the ACS Publications website at DOI: 10.1021/acs.molpharmaceut.7b00136.

NMR, HRMS, IR, fluorescence, and UV−visible spectra of the pterins **1**−**4** (PDF)

AUTHOR INFORMATION

Corresponding Authors

*Phone: 001-718-951-5658. Fax: 001-718-951-4607. E-mail: agreer@brooklyn.cuny.edu.

*Phone: +54 221 4257430 (int. 153). Fax: +54 221 4254642. E-mail: athomas@inifta.unlp.edu.ar.

ORCID

Alexander Greer: 0000-0003-4444-9099

Andrés H. Thomas: 0000-0002-8054-7799

Notes

The authors declare no competing financial interest.

ACKNOWLEDGMENTS

The authors thank the Consejo Nacional de Investigaciones Científicas y Técnicas (CONICET) and the National Science Foundation (NSF) for supporting their collaboration through a Bilateral Cooperation Programme—Level I (PCB-I, Res. 2172). N.W. and A.G. acknowledge support from the NSF (CHE-1464975). A.G. acknowledges support from the Tow Professorship at Brooklyn College. M.V. and A.H.T. acknowledge support from CONICET (Grant PIP 112-200901-00425), Agencia de Promoción Científica y Tecnológica (ANPCyT-Grant PICT-2012−0508), and Universidad Nacional de La Plata (UNLP-Grant X712). The authors gratefully acknowledge Dr. María Noel Urrutia for her contribution. M.V., S.M.B., and A.H.T. are research members of CONICET.

REFERENCES

(1) Thomas, A. H.; Catalá, Á.; Vignoni, M. Soybean phosphatidylcholine liposomes as model membranes to study lipid peroxidation photoinduced by pterin. *Biochim. Biophys. Acta, Biomembr.* **2016**, *1858* (1), 139−145.

(2) Petroselli, G.; Dántola, M. L.; Cabrerizo, F. M.; Lorente, C.; Braun, A. M.; Oliveros, E.; Thomas, A. H. Quenching of the fluorescence of aromatic pterins by deoxynucleotides. *J. Phys. Chem. A* **2009**, *113* (9), 1794−1799.

(3) Petroselli, G.; Dántola, M. L.; Cabrerizo, F. M.; Capparelli, A. L.; Lorente, C.; Oliveros, E.; Thomas, A. H. Oxidation of 2′-deoxyguanosine 5′-monophosphate photoinduced by pterin: Type I versus type II mechanism. *J. Am. Chem. Soc.* **2008**, *130* (10), 3001−3011.

(4) Dántola, M. L.; Thomas, A. H.; Braun, A. M.; Oliveros, E.; Lorente, C. Singlet oxygen ($O_2(^1\Delta_g)$) quenching by dihydropterins. *J. Phys. Chem. A* **2007**, *111* (20), 4280−4288.

(5) Folkers, K.; Laesecke, K. P. Lipoidal biopterin compounds. Google Patents: 1985.

(6) Glazer, E. C.; Nguyen, Y. H. L.; Gray, H. B.; Goodin, D. B. Probing inducible nitric oxide synthase with a pterin-ruthenium(II) sensitizer wire. *Angew. Chem., Int. Ed.* **2008**, *47* (5), 898−901.

(7) Tan, A.; Van Den Broek, L.; Bolscher, J.; Vermass, D. J.; Pastoors, L.; Van Boeckel, C.; Ploegh, H. Introduction of oxygen into the alkyl chain of N-decyl-dnm decreases lipophilicity and results in increased retention of glucose residues on N-linked oligosaccharides. *Glycobiology* **1994**, *4* (2), 141−149.

(8) Tan, A.; Van den Broek, L.; Van Boeckel, S.; Ploegh, H.; Bolscher, J. Chemical modification of the glucosidase inhibitor 1-deoxynojirimycin. Structure-activity relationships. *J. Biol. Chem.* **1991**, *266* (22), 14504−14510.

(9) Blakley, R. L. *The Biochemistry of Folic Acid and Related Pteridines*; North Holland Publishing Company: 1969.

(10) Lorente, C.; Thomas, A. H. Photophysics and photochemistry of pterins in aqueous solution. *Acc. Chem. Res.* **2006**, *39* (6), 395−402.

DOI: 10.1021/acs.molpharmaceut.7b00136
Mol. Pharmaceutics XXXX, XXX, XXX−XXX

(11) Cabrerizo, F. M.; Petroselli, G.; Lorente, C.; Capparelli, A. L.; Thomas, A. H.; Braun, A. M.; Oliveros, E. Substituent effects on the photophysical properties of pterin derivatives in acidic and alkaline aqueous solutions. *Photochem. Photobiol.* **2005**, *81* (5), 1234−1240.
(12) Crean, C. W.; Camier, R.; Lawler, M.; Stevenson, C.; Davies, R. J. H.; Boyle, P. H.; Kelly, J. M. Synthesis of N3- and 2-NH2-substituted 6,7-diphenylpterins and their use as intermediates for the preparation of oligonucleotide conjugates designed to target photo-oxidative damage on single-stranded DNA representing the bcr-abl chimeric gene. *Org. Biomol. Chem.* **2004**, *2* (24), 3588−3601.
(13) Hawkins, M. E.; Pfleiderer, W.; Jungmann, O.; Balis, F. M. Synthesis and fluorescence characterization of pteridine adenosine nucleoside analogs for DNA incorporation. *Anal. Biochem.* **2001**, *298* (2), 231−240.
(14) Baptista, M. S.; Cadet, J.; Di Mascio, P.; Ghogare, A. A.; Greer, A.; Hamblin, M. R.; Lorente, C.; Nunez, S. C.; Ribeiro, M. S.; Thomas, A. H.; Vignoni, M.; Yoshimura, T. M. Type I and II Photosensitized Oxidation Reactions: Guidelines and Mechanistic Pathways. *Photochem. Photobiol.* **2017**, DOI: 10.1111/php.12716.
(15) Greer, A.; Balaban, A. T.; Liebman, J. F. An Introduction to the Consequences of Spin and Bond Strength in the Chemistry of Diatomic Oxygen, Peroxides and Related Species. In *The Chemistry of Peroxides*; Greer, A., Liebman, J. F., Eds.; John Wiley & Sons: Chichester, U.K., 2014; Vol. 3, pp 1−20.
(16) Greer, A. Organic chemistry: Molecular cross-talk. *Nature* **2007**, *447* (7142), 273−274.
(17) Serrano, M. P.; Lorente, C.; Borsarelli, C. D.; Thomas, A. H. Unraveling the Degradation Mechanism of Purine Nucleotides Photosensitized by Pterins: The Role of Charge-Transfer Steps. *ChemPhysChem* **2015**, *16* (10), 2244−2252.
(18) Ito, K.; Kawanishi, S. Photoinduced hydroxylation of deoxyguanosine in DNA by pterins: Sequence specificity and mechanism. *Biochemistry* **1997**, *36* (7), 1774−1781.
(19) Castaño, C.; Oliveros, E.; Thomas, A. H.; Lorente, C. Histidine oxidation photosensitized by pterin: pH dependent mechanism. *J. Photochem. Photobiol., B* **2015**, *153*, 483−489.
(20) Castaño, C.; Lorente, C.; Martins-Froment, N.; Oliveros, E.; Thomas, A. H. Degradation of α-melanocyte-stimulating hormone photosensitized by pterin. *Org. Biomol. Chem.* **2014**, *12* (23), 3877−3886.
(21) Laura Dántola, M.; Zurbano, B. N.; Thomas, A. H. Photoinactivation of tyrosinase sensitized by folic acid photoproducts. *J. Photochem. Photobiol., B* **2015**, *149*, 172−179.
(22) Reid, L. O.; Roman, E. A.; Thomas, A. H.; Dántola, M. L. Photooxidation of Tryptophan and Tyrosine Residues in Human Serum Albumin Sensitized by Pterin: A Model for Globular Protein Photodamage in Skin. *Biochemistry* **2016**, *55* (34), 4777−4786.
(23) Denofrio, M. P.; Lorente, C.; Breitenbach, T.; Hatz, S.; Cabrerizo, F. M.; Thomas, A. H.; Ogilby, P. R. Photodynamic Effects of Pterin on HeLa Cells. *Photochem. Photobiol.* **2011**, *87*, 862−866.
(24) Miñán, A.; Lorente, C.; Ipiña, A.; Thomas, A. H.; Fernández Lorenzo de Mele, M.; Schilardi, P. L. Photodynamic inactivation induced by carboxypterin: a novel non-toxic bactericidal strategy against planktonic cells and biofilms of Staphylococcus aureus. *Biofouling* **2015**, *31* (5), 459−468.
(25) Mallavadhani, U. V.; Sahoo, L.; Kumar, K. P.; Murty, U. S. Synthesis and antimicrobial screening of some novel chalcones and flavanones substituted with higher alkyl chains. *Med. Chem. Res.* **2014**, *23* (6), 2900−2908.
(26) Doadrio, J. C.; Sousa, E. M. B.; Izquierdo-Barba, I.; Doadrio, A. L.; Perez-Pariente, J.; Vallet-Regi, M. Functionalization of mesoporous materials with long alkyl chains as a strategy for controlling drug delivery pattern. *J. Mater. Chem.* **2006**, *16* (5), 462−466.
(27) Nagao, Y.; Naito, T.; Abe, Y.; Misono, T. Synthesis and properties of long and branched alkyl chain substituted perylenetetracarboxylic monoanhydride monoimides. *Dyes Pigm.* **1996**, *32* (2), 71−83.
(28) Serrano, M. P.; Vignoni, M.; Dántola, M. L.; Oliveros, E.; Lorente, C.; Thomas, A. H. Emission properties of dihydropterins in aqueous solutions. *Phys. Chem. Chem. Phys.* **2011**, *13* (16), 7419−7425.
(29) Buglak, A. A.; Telegina, T. A.; Lyudnikova, T. A.; Vechtomova, Y. L.; Kritsky, M. S. Photooxidation of tetrahydrobiopterin under UV irradiation: Possible pathways and mechanisms. *Photochem. Photobiol.* **2014**, *90* (5), 1017−1026.
(30) Wilkinson, F.; Helman, H. P.; Ross, A. B. Rate Constants for the Decay and Reactions of the Lowest Electronically Excited Singlet State of Molecular Oxygen in Solution. An Expanded and Revised Compilation. *J. Phys. Chem. Ref. Data* **1995**, *24* (2), 663−667.
(31) Kuhn, H. J.; Braslavsky, S. E.; Schmidt, R. Chemical actinometry (IUPAC technical report). *Pure Appl. Chem.* **2004**, *76* (12), 2105−2146.
(32) Angeli, N. G.; Lagorio, M. G.; Román, E. A. S.; Dicelio, L. E. *Meso*-Substituted Cationic Porphyrins of Biological Interest. Photophysical and Physicochemical Properties in Solution and Bound to Liposomes. *Photochem. Photobiol.* **2000**, *72* (1), 49−56.
(33) Freccero, M.; Gandolfi, R.; Sarzi-Amadè, M. Selectivity of Purine Alkylation by a Quinone Methide. Kinetic or Thermodynamic Control? *J. Org. Chem.* **2003**, *68* (16), 6411−6423.
(34) Veldhuyzen, W. F.; Shallop, A. J.; Jones, R. A.; Rokita, S. E. Thermodynamic versus Kinetic Products of DNA Alkylation as Modeled by Reaction of Deoxyadenosine. *J. Am. Chem. Soc.* **2001**, *123* (45), 11126−11132.
(35) Babinski, D. J.; Bao, X.; El Arba, M.; Chen, B.; Hrovat, D. A.; Borden, W. T.; Frantz, D. E. Synchronized aromaticity as an enthalpic driving force for the aromatic cope rearrangement. *J. Am. Chem. Soc.* **2012**, *134* (39), 16139−16142.
(36) Schleyer, P. v. R. Introduction: Aromaticity. *Chem. Rev.* **2001**, *101* (5), 1115−1118.
(37) Langmaier, J.; Pižl, M.; Samec, Z.; Záliš, S. Extreme Basicity of Biguanide Drugs in Aqueous Solutions: Ion Transfer Voltammetry and DFT Calculations. *J. Phys. Chem. A* **2016**, *120* (37), 7344−7350.
(38) Sui, X.; Xu, Y.; Wang, X.; Han, W.; Pan, H.; Xiao, M. Metformin: A Novel but Controversial Drug in Cancer Prevention and Treatment. *Mol. Pharmaceutics* **2015**, *12* (11), 3783−3791.
(39) Matsuzaki, S.; Humphries, K. M. Selective Inhibition of Deactivated Mitochondrial Complex I by Biguanides. *Biochemistry* **2015**, *54* (11), 2011−2021.
(40) Lorenzati, B.; Zucco, C.; Miglietta, S.; Lamberti, F.; Bruno, G. Oral Hypoglycemic Drugs: Pathophysiological Basis of Their Mechanism of Action. *Pharmaceuticals* **2010**, *3* (9), 3005−3020.
(41) Kompis, I. M.; Islam, K.; Then, R. L. DNA and RNA Synthesis: Antifolates. *Chem. Rev.* **2005**, *105* (2), 593−620.
(42) http://www.schircks.ch/pteridines/data/11903_Pterin.pdf.
(43) Thomas, A. H.; Lorente, C.; Capparelli, A. L.; Pokhrel, M. R.; Braun, A. M.; Oliveros, E. Fluorescence of pterin, 6-formylpterin, 6-carboxypterin and folic acid in aqueous solution: pH effects. *Photochem. Photobiol. Sci.* **2002**, *1* (6), 421−426.
(44) Berka, V.; Yeh, H. C.; Gao, D.; Kiran, F.; Tsai, A. L. Redox function of tetrahydrobiopterin and effect of L-arginine on oxygen binding in endothelial nitric oxide synthase. *Biochemistry* **2004**, *43* (41), 13137−13148.
(45) Davis, M. D.; Kaufman, S.; Milstien, S. The auto-oxidation of tetrahydrobiopterin. *Eur. J. Biochem.* **1988**, *173* (2), 345−351.
(46) Bartholomew, R. F.; Davidson, R. S. The photosensitised oxidation of amines. Part II. The use of dyes as photosensitisers: evidence that singlet oxygen is not involved. *J. Chem. Soc. C* **1971**, *0*, 2347−2351.
(47) Kayser, R. H.; Young, R. H. The photoreduction of methylene blue by amines—II. An investigation of the decay of semireduced methylene blue. *Photochem. Photobiol.* **1976**, *24* (5), 403−411.
(48) Endo, K.; Hirayama, K.; Aota, Y.; Seya, K.; Asakura, H.; Hisamichi, K. Photooxidative decarboxylation of proline, a novel oxidative stress to natural amines. *Heterocycles* **1998**, *47* (2), 865−870.
(49) Jiang, G.; Chen, J.; Huang, J.-S.; Che, C.-M. Highly Efficient Oxidation of Amines to Imines by Singlet Oxygen and Its Application in Ugi-Type Reactions. *Org. Lett.* **2009**, *11* (20), 4568−4571.

DOI: 10.1021/acs.molpharmaceut.7b00136
Mol. Pharmaceutics XXXX, XXX, XXX−XXX

(50) Alberti, M. N.; Vougioukalakis, G. C.; Orfanopoulos, M. Photosensitized Oxidations of Substituted Pyrroles: Unanticipated Radical-Derived Oxygenated Products. *J. Org. Chem.* **2009**, *74* (19), 7274−7282.
(51) Ghogare, A. A.; Greer, A. Using Singlet Oxygen to Synthesize Natural Products and Drugs. *Chem. Rev.* **2016**, *116* (17), 9994−10034.
(52) Greer, A. Christopher Foote's discovery of the role of singlet oxygen [$^1O_2$ ($^1\Delta_g$)] in photosensitized oxidation reactions. *Acc. Chem. Res.* **2006**, *39* (11), 797−804.
(53) Calori, I. R.; Pellosi, D. S.; Vanzin, D.; Cesar, G. B.; Pereira, P. C. S.; Politi, M. J.; Hioka, N.; Caetano, W. Distribution of xanthene dyes in DPPC vesicles: Rationally accounting for drug partitioning using a membrane model. *J. Braz. Chem. Soc.* **2016**, *27* (11), 1938−1948.
(54) Jin, C. S.; Wada, H.; Anayama, T.; McVeigh, P. Z.; Hu, H. P.; Hirohashi, K.; Nakajima, T.; Kato, T.; Keshavjee, S.; Hwang, D.; Wilson, B. C.; Zheng, G.; Yasufuku, K. An Integrated Nanotechnology-Enabled Transbronchial Image-Guided Intervention Strategy for Peripheral Lung Cancer. *Cancer Res.* **2016**, *76* (19), 5870−5880.
(55) Valic, M. S.; Zheng, G. Rethinking translational nanomedicine: insights from the 'bottom-up' design of the Porphysome for guiding the clinical development of imageable nanomaterials. *Curr. Opin. Chem. Biol.* **2016**, *33*, 126−134.
(56) Ng, K. K.; Takada, M.; Jin, C. C. S.; Zheng, G. Self-Sensing Porphysomes for Fluorescence-Guided Photothermal Therapy. *Bioconjugate Chem.* **2015**, *26* (2), 345−351.
(57) MacDonald, T. D.; Zheng, G. Porphysome nanoparticles: Tailoring treatments with nature's pigments. *Photonics Lasers Med.* **2014**, *3* (3), 183−191.
(58) Lovell, J. F.; Jin, C. S.; Huynh, E.; Jin, H.; Kim, C.; Rubinstein, J. L.; Chan, W. C. W.; Cao, W.; Wang, L. V.; Zheng, G. Porphysome nanovesicles generated by porphyrin bilayers for use as multimodal biophotonic contrast agents. *Nat. Mater.* **2011**, *10* (4), 324−332.

DOI: 10.1021/acs.molpharmaceut.7b00136
Mol. Pharmaceutics XXXX, XXX, XXX−XXX